

World Journal of *Gastrointestinal Oncology*

World J Gastrointest Oncol 2024 April 15; 16(4): 1091-1675



EDITORIAL

- 1091 Parallel pathways: A chronicle of evolution in rectal and breast cancer surgery
Pesce A, Fabbri N, Iovino D, Feo CV
- 1097 Hepatitis B virus genotypes in precision medicine of hepatitis B-related hepatocellular carcinoma: Where we are now
Sukowati CHC, Jayanti S, Turyadi T, Muljono DH, Tiribelli C

REVIEW

- 1104 Novel milestones for early esophageal carcinoma: From bench to bed
Qi JH, Huang SL, Jin SZ
- 1119 Colorectal cancer screening: A review of current knowledge and progress in research
Lopes SR, Martins C, Santos IC, Teixeira M, Gamito É, Alves AL
- 1134 New avenues for the treatment of immunotherapy-resistant pancreatic cancer
Silva LGO, Lemos FFB, Luz MS, Rocha Pinheiro SL, Calmon MDS, Correa Santos GL, Rocha GR, de Melo FF

MINIREVIEWS

- 1154 Present situation of minimally invasive surgical treatment for early gastric cancer
Li CY, Wang YF, Luo LK, Yang XJ
- 1166 Mixed neuroendocrine non-neuroendocrine neoplasms in gastroenteropancreatic tract
Díaz-López S, Jiménez-Castro J, Robles-Barraza CE, Ayala-de Miguel C, Chaves-Conde M
- 1180 Esophageal cancer screening, early detection and treatment: Current insights and future directions
Qu HT, Li Q, Hao L, Ni YJ, Luan WY, Yang Z, Chen XD, Zhang TT, Miao YD, Zhang F

ORIGINAL ARTICLE**Retrospective Cohort Study**

- 1192 Pre-operative enhanced magnetic resonance imaging combined with clinical features predict early recurrence of hepatocellular carcinoma after radical resection
Chen JP, Yang RH, Zhang TH, Liao LA, Guan YT, Dai HY
- 1204 Clinical analysis of multiple primary gastrointestinal malignant tumors: A 10-year case review of a single-center
Zhu CL, Peng LZ

Retrospective Study

- 1213** Predictive model for non-malignant portal vein thrombosis associated with cirrhosis based on inflammatory biomarkers
Nie GL, Yan J, Li Y, Zhang HL, Xie DN, Zhu XW, Li X
- 1227** Predictive modeling for postoperative delirium in elderly patients with abdominal malignancies using synthetic minority oversampling technique
Hu WJ, Bai G, Wang Y, Hong DM, Jiang JH, Li JX, Hua Y, Wang XY, Chen Y
- 1236** Efficacy and predictive factors of transarterial chemoembolization combined with lenvatinib plus programmed cell death protein-1 inhibition for unresectable hepatocellular carcinoma
Ma KP, Fu JX, Duan F, Wang MQ
- 1248** Should we perform sigmoidoscopy for colorectal cancer screening in people under 45 years?
Leong W, Guo JQ, Ning C, Luo FF, Jiao R, Yang DY
- 1256** Computed tomography-based radiomics diagnostic approach for differential diagnosis between early- and late-stage pancreatic ductal adenocarcinoma
Ren S, Qian LC, Cao YY, Daniels MJ, Song LN, Tian Y, Wang ZQ
- 1268** Prognostic analysis of related factors of adverse reactions to immunotherapy in advanced gastric cancer and establishment of a nomogram model
He XX, Du B, Wu T, Shen H

Clinical Trials Study

- 1281** Safety and efficacy of a programmed cell death 1 inhibitor combined with oxaliplatin plus S-1 in patients with Borrmann large type III and IV gastric cancers
Bao ZH, Hu C, Zhang YQ, Yu PC, Wang Y, Xu ZY, Fu HY, Cheng XD

Observational Study

- 1296** Computed tomography radiogenomics: A potential tool for prediction of molecular subtypes in gastric stromal tumor
Yin XN, Wang ZH, Zou L, Yang CW, Shen CY, Liu BK, Yin Y, Liu XJ, Zhang B
- 1309** Application of texture signatures based on multiparameter-magnetic resonance imaging for predicting microvascular invasion in hepatocellular carcinoma: Retrospective study
Nong HY, Cen YY, Qin M, Qin WQ, Xie YX, Li L, Liu MR, Ding K
- 1319** Causal roles of gut microbiota in cholangiocarcinoma etiology suggested by genetic study
Chen ZT, Ding CC, Chen KL, Gu YJ, Lu CC, Li QY
- 1334** Is recovery enhancement after gastric cancer surgery really a safe approach for elderly patients?
Li ZW, Luo XJ, Liu F, Liu XR, Shu XP, Tong Y, Lv Q, Liu XY, Zhang W, Peng D
- 1344** Establishment of a cholangiocarcinoma risk evaluation model based on mucin expression levels
Yang CY, Guo LM, Li Y, Wang GX, Tang XW, Zhang QL, Zhang LF, Luo JY

- 1361** Effectiveness of fecal DNA syndecan-2 methylation testing for detection of colorectal cancer in a high-risk Chinese population

Luo WF, Jiao YT, Lin XL, Zhao Y, Wang SB, Shen J, Deng J, Ye YF, Han ZP, Xie FM, He JH, Wan Y

Clinical and Translational Research

- 1374** Clinical and socioeconomic determinants of survival in biliary tract adenocarcinomas

Sahyoun L, Chen K, Tsay C, Chen G, Protiva P

- 1384** Risk factors, prognostic factors, and nomograms for distant metastasis in patients with diagnosed duodenal cancer: A population-based study

Shang JR, Xu CY, Zhai XX, Xu Z, Qian J

- 1421** NOX4 promotes tumor progression through the MAPK-MEK1/2-ERK1/2 axis in colorectal cancer

Xu YJ, Huo YC, Zhao QT, Liu JY, Tian YJ, Yang LL, Zhang Y

Basic Study

- 1437** Curcumin inhibits the growth and invasion of gastric cancer by regulating long noncoding RNA AC022424.2

Wang BS, Zhang CL, Cui X, Li Q, Yang L, He ZY, Yang Z, Zeng MM, Cao N

- 1453** MicroRNA-298 determines the radio-resistance of colorectal cancer cells by directly targeting human dual-specificity tyrosine(Y)-regulated kinase 1A

Shen MZ, Zhang Y, Wu F, Shen MZ, Liang JL, Zhang XL, Liu XJ, Li XS, Wang RS

- 1465** Human β -defensin-1 affects the mammalian target of rapamycin pathway and autophagy in colon cancer cells through long non-coding RNA TCONS_00014506

Zhao YX, Cui Y, Li XH, Yang WH, An SX, Cui JX, Zhang MY, Lu JK, Zhang X, Wang XM, Bao LL, Zhao PW

- 1479** FAM53B promotes pancreatic ductal adenocarcinoma metastasis by regulating macrophage M2 polarization

Pei XZ, Cai M, Jiang DW, Chen SH, Wang QQ, Lu HM, Lu YF

- 1500** Transcriptome sequencing reveals novel biomarkers and immune cell infiltration in esophageal tumorigenesis

Sun JR, Chen DM, Huang R, Wang RT, Jia LQ

- 1514** Construction of CDKN2A-related competitive endogenous RNA network and identification of GAS5 as a prognostic indicator for hepatocellular carcinoma

Pan Y, Zhang YR, Wang LY, Wu LN, Ma YQ, Fang Z, Li SB

- 1532** Two missense *STK11* gene variations impaired LKB1/adenosine monophosphate-activated protein kinase signaling in Peutz-Jeghers syndrome

Liu J, Zeng SC, Wang A, Cheng HY, Zhang QJ, Lu GX

- 1547** Long noncoding RNAs HAND2-AS1 ultrasound microbubbles suppress hepatocellular carcinoma progression by regulating the miR-873-5p/tissue inhibitor of matrix metalloproteinase-2 axis

Zou Q, Wang HW, Di XL, Li Y, Gao H

- 1564** Upregulated lncRNA PRNT promotes progression and oxaliplatin resistance of colorectal cancer cells by regulating HIPK2 transcription

Li SN, Yang S, Wang HQ, Hui TL, Cheng M, Zhang X, Li BK, Wang GY

SYSTEMATIC REVIEWS

- 1578** Prognosis value of heat-shock proteins in esophageal and esophagogastric cancer: A systematic review and meta-analysis

Nakamura ET, Park A, Pereira MA, Kikawa D, Tustumi F

- 1596** Risk factors for hepatocellular carcinoma associated with hepatitis C genotype 3 infection: A systematic review

Farooq HZ, James M, Abbott J, Oyibo P, Divall P, Choudhry N, Foster GR

META-ANALYSIS

- 1613** Effectiveness and tolerability of programmed cell death protein-1 inhibitor + chemotherapy compared to chemotherapy for upper gastrointestinal tract cancers

Zhang XM, Yang T, Xu YY, Li BZ, Shen W, Hu WQ, Yan CW, Zong L

- 1626** Success rate of current human-derived gastric cancer organoids establishment and influencing factors: A systematic review and meta-analysis

Jiang KL, Wang XX, Liu XJ, Guo LK, Chen YQ, Jia QL, Yang KM, Ling JH

CASE REPORT

- 1647** Pathologically successful conversion hepatectomy for advanced giant hepatocellular carcinoma after multidisciplinary therapy: A case report and review of literature

Chu JH, Huang LY, Wang YR, Li J, Han SL, Xi H, Gao WX, Cui YY, Qian MP

- 1660** Clinical pathological characteristics of “crawling-type” gastric adenocarcinoma cancer: A case report

Xu YW, Song Y, Tian J, Zhang BC, Yang YS, Wang J

- 1668** Primary pancreatic peripheral T-cell lymphoma: A case report

Bai YL, Wang LJ, Luo H, Cui YB, Xu JH, Nan HJ, Yang PY, Niu JW, Shi MY

ABOUT COVER

Peer Reviewer of *World Journal of Gastrointestinal Oncology*, Lie Zheng, Director, Professor, Department of Gastroenterology, Shaanxi Provincial Hospital of Traditional Chinese Medicine, Xi'an 730000, Shaanxi Province, China. xinliwen696@126.com

AIMS AND SCOPE

The primary aim of *World Journal of Gastrointestinal Oncology (WJGO, World J Gastrointest Oncol)* is to provide scholars and readers from various fields of gastrointestinal oncology with a platform to publish high-quality basic and clinical research articles and communicate their research findings online.

WJGO mainly publishes articles reporting research results and findings obtained in the field of gastrointestinal oncology and covering a wide range of topics including liver cell adenoma, gastric neoplasms, appendiceal neoplasms, biliary tract neoplasms, hepatocellular carcinoma, pancreatic carcinoma, cecal neoplasms, colonic neoplasms, colorectal neoplasms, duodenal neoplasms, esophageal neoplasms, gallbladder neoplasms, *etc.*

INDEXING/ABSTRACTING

The *WJGO* is now abstracted and indexed in PubMed, PubMed Central, Science Citation Index Expanded (SCIE, also known as SciSearch®), Journal Citation Reports/Science Edition, Scopus, Reference Citation Analysis, China Science and Technology Journal Database, and Superstar Journals Database. The 2023 edition of Journal Citation Reports® cites the 2022 impact factor (IF) for *WJGO* as 3.0; IF without journal self cites: 2.9; 5-year IF: 3.0; Journal Citation Indicator: 0.49; Ranking: 157 among 241 journals in oncology; Quartile category: Q3; Ranking: 58 among 93 journals in gastroenterology and hepatology; and Quartile category: Q3. The *WJGO*'s CiteScore for 2022 is 4.1 and Scopus CiteScore rank 2022: Gastroenterology is 71/149; Oncology is 197/366.

RESPONSIBLE EDITORS FOR THIS ISSUE

Production Editor: *Xiang-Di Zhang*; **Production Department Director:** *Xiang Li*; **Cover Editor:** *Jia-Ru Fan*.

NAME OF JOURNAL

World Journal of Gastrointestinal Oncology

ISSN

ISSN 1948-5204 (online)

LAUNCH DATE

February 15, 2009

FREQUENCY

Monthly

EDITORS-IN-CHIEF

Monjur Ahmed, Florin Burada

EDITORIAL BOARD MEMBERS

<https://www.wjgnet.com/1948-5204/editorialboard.htm>

PUBLICATION DATE

April 15, 2024

COPYRIGHT

© 2024 Baishideng Publishing Group Inc

INSTRUCTIONS TO AUTHORS

<https://www.wjgnet.com/bpg/gerinfo/204>

GUIDELINES FOR ETHICS DOCUMENTS

<https://www.wjgnet.com/bpg/GerInfo/287>

GUIDELINES FOR NON-NATIVE SPEAKERS OF ENGLISH

<https://www.wjgnet.com/bpg/gerinfo/240>

PUBLICATION ETHICS

<https://www.wjgnet.com/bpg/GerInfo/288>

PUBLICATION MISCONDUCT

<https://www.wjgnet.com/bpg/gerinfo/208>

ARTICLE PROCESSING CHARGE

<https://www.wjgnet.com/bpg/gerinfo/242>

STEPS FOR SUBMITTING MANUSCRIPTS

<https://www.wjgnet.com/bpg/GerInfo/239>

ONLINE SUBMISSION

<https://www.f6publishing.com>



Clinical and Translational Research

NOX4 promotes tumor progression through the MAPK-MEK1/2-ERK1/2 axis in colorectal cancer

Yu-Jie Xu, Ya-Chang Huo, Qi-Tai Zhao, Jin-Yan Liu, Yi-Jun Tian, Lei-Lei Yang, Yi Zhang

Specialty type: Oncology

Provenance and peer review:

Unsolicited article; Externally peer reviewed.

Peer-review model: Single blind

Peer-review report's scientific quality classification

Grade A (Excellent): 0

Grade B (Very good): B

Grade C (Good): 0

Grade D (Fair): 0

Grade E (Poor): 0

P-Reviewer: Tchilikidi KY, Russia

Received: December 8, 2023

Peer-review started: December 8, 2023

First decision: December 21, 2023

Revised: January 4, 2024

Accepted: February 7, 2024

Article in press: February 7, 2024

Published online: April 15, 2024



Yu-Jie Xu, Ya-Chang Huo, Qi-Tai Zhao, Jin-Yan Liu, Yi-Jun Tian, Lei-Lei Yang, Yi Zhang, Biotherapy Center and Cancer Center, The First Affiliated Hospital of Zhengzhou University, Zhengzhou 450052, Henan Province, China

Yu-Jie Xu, Department of Oncology, Henan Provincial People's Hospital, People's Hospital of Zhengzhou University, People's Hospital of Henan University, Zhengzhou 450003, Henan Province, China

Corresponding author: Yi Zhang, MD, PhD, Chief Physician, Full Professor, Biotherapy Center and Cancer Center, The First Affiliated Hospital of Zhengzhou University, No. 1 Jianshe East Road, Zhengzhou 450052, Henan Province, China. yizhang@zzu.edu.cn

Abstract

BACKGROUND

Metabolic reprogramming plays a key role in cancer progression and clinical outcomes; however, the patterns and primary regulators of metabolic reprogramming in colorectal cancer (CRC) are not well understood.

AIM

To explore the role of nicotinamide adenine dinucleotide phosphate oxidase 4 (NOX4) in promoting progression of CRC.

METHODS

We evaluated the expression and function of dysregulated and survival-related metabolic genes using Gene Ontology and Kyoto Encyclopedia of Genes and Genomes. Consensus clustering was used to cluster CRC based on dysregulated metabolic genes. A prediction model was constructed based on survival-related metabolic genes. Sphere formation, migration, invasion, proliferation, apoptosis and clone formation was used to evaluate the biological function of NOX4 in CRC. mRNA sequencing was utilized to explore the alterations of gene expression NOX4 over-expression tumor cells. *In vivo* subcutaneous and lung metastasis mouse tumor model was used to explore the effect of NOX4 on tumor growth.

RESULTS

We comprehensively analyzed 3341 metabolic genes in CRC and identified three clusters based on dysregulated metabolic genes. Among these genes, NOX4 was highly expressed in tumor tissues and correlated with worse survival. *In vitro*, NOX4 overexpression induced clone formation, migration, invasion, and

stemness in CRC cells. Furthermore, RNA-sequencing analysis revealed that NOX4 overexpression activated the mitogen-activated protein kinase-MEK1/2-ERK1/2 signaling pathway. Trametinib, a MEK1/2 inhibitor, abolished the NOX4-mediated tumor progression. *In vivo*, NOX4 overexpression promoted subcutaneous tumor growth and lung metastasis, whereas trametinib treatment can reversed the metastasis.

CONCLUSION

Our study comprehensively analyzed metabolic gene expression and highlighted the importance of NOX4 in promoting CRC metastasis, suggesting that trametinib could be a potential therapeutic drugs of CRC clinical therapy targeting NOX4.

Key Words: Colorectal cancer; Metabolic reprogramming; Metastasis; Nicotinamide adenine dinucleotide phosphate oxidase 4; Mitogen-activated protein kinase signaling

©The Author(s) 2024. Published by Baishideng Publishing Group Inc. All rights reserved.

Core Tip: We first identified three clusters with different survival status based on dysregulated metabolic genes in colorectal cancer (CRC). In addition, based on differentially expressed survival-related metabolic genes, we constructed and validated a prediction model using different cohorts. Among these genes, nicotinamide adenine dinucleotide phosphate oxidase 4 (NOX4) overexpression activated the mitogen-activated protein kinase-MEK1/2-ERK1/2 signaling pathway to promote cancer metastasis, whereas trametinib (a MEK1/2 inhibitor) treatment reversed this effect. Our study analyzed metabolic gene expression and highlighted the importance of NOX4 in promoting CRC metastasis, suggesting that NOX4 could be a new therapeutic target and modulating the response to clinical therapy.

Citation: Xu YJ, Huo YC, Zhao QT, Liu JY, Tian YJ, Yang LL, Zhang Y. NOX4 promotes tumor progression through the MAPK-MEK1/2-ERK1/2 axis in colorectal cancer. *World J Gastrointest Oncol* 2024; 16(4): 1421-1436

URL: <https://www.wjgnet.com/1948-5204/full/v16/i4/1421.htm>

DOI: <https://dx.doi.org/10.4251/wjgo.v16.i4.1421>

INTRODUCTION

Colorectal cancer (CRC) is the third most common cause of cancer-related death, accounting for approximately 10% of all cancers diagnosed worldwide[1]. For early CRC, treatment options include endoscopic and surgical approaches, while for patients with advanced stage CRC, such as fluoropyrimidine-based chemotherapy, radiotherapy, have been used to improve the survival rate[2-5]. In addition, targeted therapies and immunotherapies have been used to treat advanced and metastatic CRC[6,7]. However, the majority of patients do not respond to these therapies[8]. This outcome is partially due to the tumor metabolic reprogramming.

Metabolic reprogramming is a hallmark of cancer and is responsible for the ability of tumor cells to evade drug therapy [9,10]. The first recognized concept of metabolic reprogramming was called Warburg effect[11]. Warburg effect is the enhanced conversion of glucose to pyruvate even in the presence of abundant oxygen[12]. Additionally, in KRAS-mutant CRC, solute carrier family 7, member 5 maintains intracellular amino acid levels required for tumor growth[13]. V-9302, an antagonist of SLC1A5, was reported to reduce tumor growth in the mouse models of breast and liver cancers[14,15]. To date, numerous metabolic genes have been identified as potential drug candidates; however, off-target side effects and metabolic plasticity add to the challenges of drug development. Thus, a comprehensive understanding of the metabolic patterns and identification of key molecules in CRC are essential for targeting cancer metabolism.

Nicotinamide adenine dinucleotide phosphate oxidase 4 (NOX4) is an aberrantly-expressed metabolic gene that correlated with tumor progression. NOX4 belongs to the NOX family, and is the major oxidase involved in the production of reactive oxygen species (ROS)[16]. NOX4 is widely expressed and is involved in the regulation of numerous cell functions[17,18]. Furthermore, it has been proposed that an equilibrium between the production and elimination of ROS is required for the initiation and progression of cancer[16], suggesting that the expression of NOX4 is linked to tumor progression.

Here, we performed a comprehensive analysis of aberrant expression of metabolic gene and signaling pathways involved in CRC, and further classified the patients into three clusters based on different metabolic gene patterns. A prediction model was constructed to predict survival of patients with CRC based on survival-related genes. We found that NOX4 overexpression promoted CRC progression and metastasis *via* mitogen-activated protein kinase (MAPK)-MEK1/2-ERK1/2 signaling.

MATERIALS AND METHODS

Data collection and analysis

The RNA sequencing data and corresponding clinical information of CRC samples from The Cancer Genome Atlas (TCGA) Program were downloaded from the online database UCSC Xena (xena.ucsc.edu) with $\log_2(\text{RSEM} + 1)$ format. Metabolic genes were selected by integrating two previously published datasets[19,20]. The colon cancer microarray expression data and corresponding clinical information were downloaded from the Gene Expression Omnibus (GEO) database (<https://www.ncbi.nlm.nih.gov/geo/>) with accession number GSE17536.

Identification of differentially expressed genes and gene function enrichment analysis

The R package “limma” was used to identify the metabolic differentially expressed genes (DEGs) between CRC and normal tissues, and the genes with an adjusted P -value < 0.05 and \log_2 -fold change $|\log_2 \text{FC}| > 1$ were visualized using a volcano map. The top ten dysregulated metabolic genes (ranked by adjusted P -value) were analyzed using the R package “ggplot2”. The R packages “clusterProfiler”, “org.Hs.eg.db”, and “enrichplot” were used to perform Gene Ontology (GO) and Kyoto Encyclopedia of Genes and Genomes (KEGG) of DEGs, and significantly enrichment GO and KEGG categories (P -value < 0.05 and q -value < 0.05) were selected.

Consensus clustering and characterization of CRC based on metabolic DEGs

The R package “ConsensusClusterPlus” was used to cluster CRC based on metabolic DEGs. Clusters were visualized using “pheatmap”. Pie and bar plots were used to display patient clinical parameters and the R package “survival” was used to analyze differences of overall survival (OS) and progression free interval (PFI) across the three clusters.

Construction and validation of prediction model

Tumor samples from TCGA were randomly divided into training and test groups in a 1:1 ratio based on survival status. Univariate survival analysis was performed for each gene to select candidate metabolic genes related to OS in the training datasets. The least absolute shrinkage and selection operator (Lasso) algorithm was used to optimize the gene signatures, and multivariate Cox regression analysis was used to calculate the formula for the prediction model. The R packages “survival”, “survminer”, and “survival ROC” were used to analyze the differences of survival and receiver operating characteristic (ROC) curve between high- and low-risk groups. Only gene signatures from prediction model were used for validating in our clinical samples and GEO datasets.

Clinical specimens

Pairs of freshly frozen samples of primary CRC and adjacent tumor tissues ($n = 82$) were obtained from patients who underwent surgical resection at the First Affiliated Hospital of Zhengzhou University. None of the patients received preoperative chemotherapy, radiotherapy, or other tumor-specific treatments. Total of 82 patients were followed up through an interview at the clinic or by telephone. The clinicopathological parameters of patients with CRC are summarized in [Table 1](#).

Cell culture and lentiviral transfection

CRC cell line RKO was cultured in the DMEM (Dulbecco’s Modified Eagle’s Medium-high glucose) (Sigma, United States) supplemented with 10% fetal bovine serum, 100 U/mL penicillin and 100 $\mu\text{g}/\text{mL}$ streptomycin in a 5% CO_2 atmosphere at 37 °C. To overexpress NOX4 in RKO cells, the target gene fragment was amplified using the primers listed in [Supplementary Table 1](#). The fragment was cloned into the lentiviral vector Ubi-MCS-3FLAG-CBh-gcGFP-IRES-puromycin (GeneChem Co., Ltd., Shanghai, China). Next, lentiviruses containing the target fragment or negative control were transfected into RKO cells. After 72 h, NOX4-overexpressing RKO cells were selected with puromycin (2 $\mu\text{g}/\text{mL}$; Santa Cruz).

RNA extraction and real-time quantitative polymerase chain reaction

Total RNA was extracted using the Trizol reagent, and 1 μg of total RNA was reverse-transcribed using the PrimeScript RT-PCR kit (Takara, Japan). Real-time quantitative polymerase chain reaction (RT-qPCR, Applied Biosystems, Grand Island, NY, United States) was performed using the SYBR Green method (Takara, Japan). The $2^{-\Delta\Delta\text{Ct}}$ method was used to quantify the relative NOX4 expression levels. The primers used for RT-PCR were listed in [Supplementary Table 2](#).

Western blot analysis

Whole cell lysates were prepared using RIPA lysis buffer containing a protease inhibitor cocktail (Sigma-Aldrich) and phosphatase inhibitor cocktail 2 (Sigma-Aldrich). Equal amounts of protein were loaded onto a 10% sodium-dodecyl sulfate gel electrophoresis gel and then transferred to a polyvinylidene fluoride membrane (Bio-Rad, Hercules, CA, United States). Membranes were blocked in 5% nonfat milk and incubated with primary antibodies overnight at 4 °C, followed by treatment with secondary antibody for 2 h at 37 °C. The primary antibodies were NOX4 (1:1000, ab133303, Abcam), phospho-p44/42 MAPK (Erk1/2) (1:2000, 4370T, Cell Signaling Technology), p44/42 MAPK (Erk1/2) (1:1000, 4695T, Cell Signaling Technology), MEK1/2 (1:1000, 8727T, Cell Signaling Technology), phospho-MEK1/2 (1:1000, 9154T, Cell Signaling Technology), β -actin (1:5000, 4967S, Cell Signaling Technology). Blots were imaged using enhanced chemiluminescence (Thermo Fisher, United States).

Table 1 Basic information of patients and its relationship with nicotinamide adenine dinucleotide phosphate oxidase 4

Factor	Category	Total	High NOX4 (N = 52)	Low NOX4 (N = 30)	P value
Age (yr)		64.46 ± 12.6	64.79 ± 12.38	63.9 ± 13.18	0.765
Gender	Female	49 (60)	31 (60)	18 (60)	1.000
	Male	33 (40)	21 (40)	12 (40)	
Tumor location	Left colon or rectum	51 (62)	35 (67)	16 (53)	0.307
	Right colon	31 (38)	17 (33)	14 (47)	
Histopathology	Well differentiated	31 (38)	17 (33)	14 (47)	0.373
	Moderately differentiated	32 (39)	23 (44)	9 (30)	
	Poorly differentiated	19 (23)	12 (23)	7 (23)	
pT	T1	17 (21)	11 (21)	6 (20)	0.357
	T2	26 (32)	13 (25)	13 (43)	
	T3	24 (29)	17 (33)	7 (23)	
	T4	15 (18)	11 (21)	4 (13)	
pN	N0	45 (55)	25 (48)	20 (67)	0.233
	N1	26 (32)	18 (35)	8 (27)	
	N2	11 (13)	9 (17)	2 (7)	
pM	M0	82 (100)	52 (100)	30 (100)	1.000
	M1	0	0	0	
pStage	Stage I	19 (23)	5 (10)	14 (47)	< 0.001
	Stage II	24 (29)	19 (37)	5 (17)	
	Stage III	39 (48)	28 (54)	11 (37)	

NOX4: Nicotinamide adenine dinucleotide phosphate oxidase 4.

Immunofluorescence staining

NOX4-overexpressing and negative control RKO cells were permeabilized with 0.3% Triton X-100 for 10 min and then washed. The sections were incubated with primary antibodies anti-NOX4 (1:500, Abcam) and anti-p-ERK (1:200, Abcam) overnight at 4 °C. Fluorescein isothiocyanate and Cy3-conjugated secondary antibodies (1:500, BioLegend) were used to detect the primary antibodies. The stained cells were counterstained with 4'6-diamidino-2-phenylindole (1:1000; Roche, Basel, Switzerland) and analyzed using an IX71 inverted fluorescence microscope (model 1003; Olympus).

Immunohistochemical staining

CRC tissues and corresponding adjacent tissues were evaluated for NOX4 and p-Erk expression using immunohistochemical (IHC) staining. Sections were treated with 3% hydrogen peroxide and 5% BSA, and then incubated with primary antibodies (NOX4, 1:100, Abcam, Cambridge; p-Erk, 1:200, Abcam) overnight at 4 °C. Next, the sections were incubated with horseradish peroxidase-conjugated secondary antibody for 1 h at 37 °C, counterstained with hematoxylin, and then visualized under a microscope (Olympus, Tokyo, Japan). NOX4 staining was semi-quantitatively evaluated using a grading system based on staining intensity (scored as follows: 0, no staining; 1, weak staining; 2, moderate staining; 3, strong staining) and the percentage of positive tumor cells (scored as follows: 0, none; 1, 1%-29%; 2, 30%-69%; 3, > 70%). The total IHC score for each tissue sample was calculated by multiplying the staining intensity score by the positive tumor cell score. The final score, which ranged from 0 to 9 was defined as follows: 0, negative (-); 1-3 (+), weak; 4-6 (++) , moderate; and > 6, strong (+++).

Transwell migration and invasion assays

The migration and invasion of NOX4-overexpressing and negative control RKO cells were evaluated using transwell assays. Briefly, 2 × 10⁶ cells/well were cultured in foetal bovine serum-free DMEM in the upper chambers of a 8.0 µm pore transwell insert (Corning, United States) and treated with either MEK inhibitor (MEKi, trametinib, 100 nM) or vehicle control. For the invasion assay, the upper chambers of transwell plates were pre-coated with 40 µL Matrigel (1:8 dilution, BD Biosciences) at 37 °C for 30 min for gelling. Cells were cultured for 36 h, fixed with 4% paraformaldehyde (Sigma-Aldrich; Merck KGaA) at 37 °C for 20 min, and then stained with 0.5% crystal violet (Sigma-Aldrich; Merck KGaA) at 37 °C for 15 min. The number of invaded cells was counted under an optical microscope at 100 × magnification (five random fields per sample).

Cell proliferation, cell-cycle, and apoptosis assays

Cell viability of NOX4-overexpressing and negative-control RKO cells was evaluated using the cell counting kit-8 (CCK8, Dojindo Molecular Technologies, Japan). Briefly, the RKO cells were seeded into 96-well plates at a density of 5×10^3 cells/well. CCK8 solution was added to each well at 24, 48, and 72 h, and cells were incubated for 30 min at 37 °C. Absorbance at 450 nm was measured using a microplate reader (spectraMax iD3, PerkinElmer, United States). The cell cycle was examined using propidium iodide (PI) (BD Biosciences) staining. Cells were washed with cold phosphate buffered saline (PBS), fixed in 75% ethanol at -20 °C overnight, incubated with PI for 15 min, and then analyzed using flow cytometry.

Wound healing analysis

NOX4-overexpressing and negative control RKO cells were seeded into 6-well plates at a density of 1×10^6 cells/well. Next, three evenly-spaced vertical lines were made in each well using a 200 μ L enzyme-free yellow pipette tip. The culture medium was then removed, wells were washed three times with PBS, and 2 mL of serum-free DMEM was slowly added. Images at 0, 24, and 48 h time points were obtained using an optical microscope at 100 \times magnification.

Cell colonizing experiment

NOX4-overexpressing and negative control RKO cells were seeded into the 6-well plates at a density of 1×10^3 cells/mL and incubated in a 5% CO₂ atmosphere at 37 °C. When the cell clones in the wells were visible by eye, the cells were fixed with 4% paraformaldehyde (Sigma-Aldrich; Merck KGaA) at 37 °C for 20 min, stained with 0.5% crystal violet (Sigma-Aldrich; Merck KGaA) at 37 °C for 15 min, and the number of invaded cells was counted under an optical microscope.

Sphere formation analysis

NOX4-overexpressing and negative-control-RKO cells were seeded into low adhesion 6-well plates at a density of 2×10^3 cells/mL and then cultured in tumor sphere formation medium [DMEM/F12 + basic fibroblast growth factor (20 ng/mL) + epidermal growth factor (20 ng/mL) + B27 (1:50) + Heparin (4 mg/mL)] in a 5% CO₂ atmosphere at 37 °C for 5-7 d. The number of tumor spheres was counted using an optical microscope.

RNA-sequencing analysis

RNA-sequencing analysis were conducted by SeqHealth Technology Co., LTD (Wuhan, China). Principal component analysis was performed using the R packages “FactoMineR” and “ggplot2”. “Limma” was used to identify DEGs and the results were visualized using volcano and pheatmap plots. “ClusterProfiler” was used to perform GO and KEGG analyses of the DEGs.

In vivo tumor experiments and treatments

Female BALB/c nude mice (5-6 wk-old) were purchased from Vital River Laboratory Animal Technology Co. Ltd. (Beijing, China). The mice were housed under pathogen-free conditions. To generate a xenograft mouse model mice were randomly divided into two groups ($n = 6$ /group). NOX4-overexpressing and negative control RKO cells (5×10^6) were injected subcutaneously and intravenously. Tumor volume was evaluated every 3 d using digital calipers. Next, the mice were intravenously treated with: (1) trametinib (1 mg/kg, daily; $n = 3$); or (2) Vehicle control ($n = 3$) at day 14. At day 28, mice were sacrificed, and the tumors and lungs were harvested for further analysis. All animal experiments were approved by the Institutional Animal Care and Use Committee of the First Affiliated Hospital of Zhengzhou University, China.

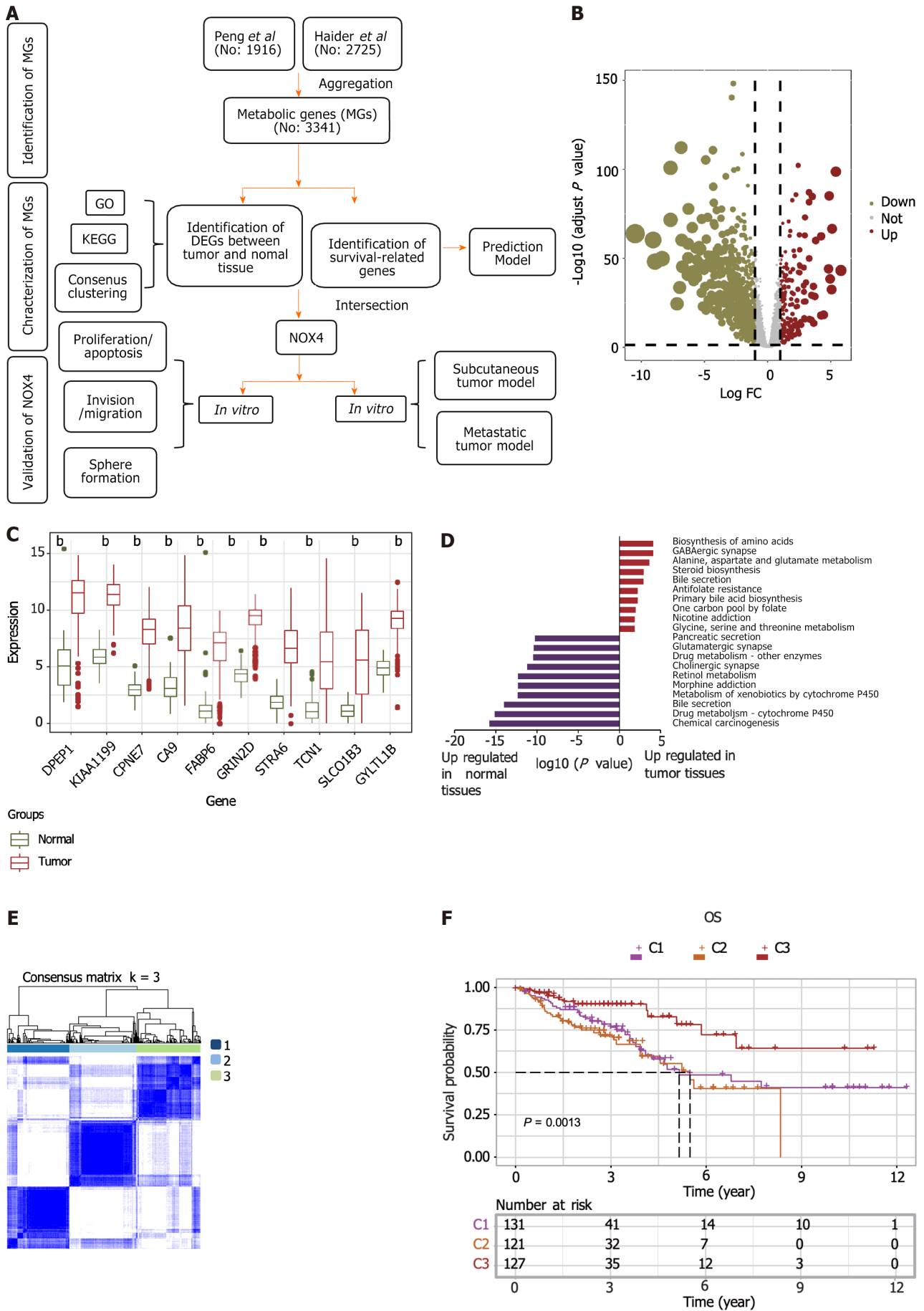
Statistical analysis

Statistical analysis was performed using the R software (version 4.0.1) and GraphPad Prism (version 9). Two-tailed unpaired or paired *t*-tests were used to compare the differences between two groups *in vitro* experiments, the Wilcoxon test was used to compare the differences between two groups in the bioinformatic analysis, and analysis of variance (ANOVA) was used to compare the differences between more than two groups, data were showed by mean \pm SEM. $P < 0.05$ was considered statistically significant.

RESULTS

Identification of dysregulated metabolic genes in CRC tissues

To evaluate the expression of metabolic genes in CRC, we integrated two published metabolic datasets and performed a multistep analysis (Figure 1A). Total of 3341 metabolic genes were selected, of which 942 DEGs were identified dysregulated in tumor and adjacent normal tissues (726 genes were upregulated in tumor tissues and 216 genes were downregulated) (Figure 1B). The top ten DEGs, as shown in a boxplot, were all upregulated in tumor tissues (Figure 1C). The top five KEGG signaling pathways for the upregulated DEGs enrichment were: Biosynthesis of amino acids; GABAergic synapse; alanine, aspartate, and glutamate metabolism; steroid biosynthesis and bile secretion. The downregulated DEGs were enriched in chemical carcinogenesis, drug metabolism-cytochrome P450, bile secretion, xenobiotic metabolism by cytochrome P450, morphine addiction, and retinol metabolism (Figure 1D). The GO annotation results revealed that the upregulated DEGs were primarily enriched in the transmembrane transporter activity of anions and metabolites, whereas the downregulated genes were involved in the channel activity of ions, as well as transmembrane transporter activity



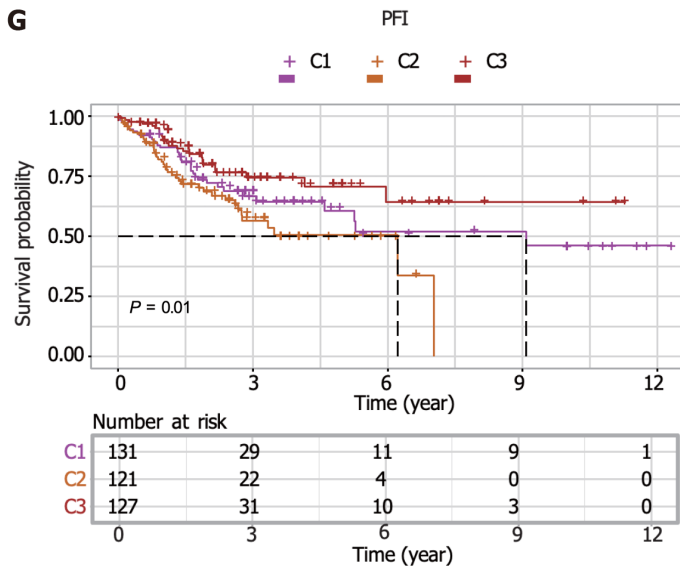


Figure 1 Identification of dysregulated metabolic genes in tumor tissues. A: Multi-step analysis of metabolic genes in this study; B: Volcano plot showing metabolic differentially expressed genes (DEGs) between tumor and adjacent tissues; C: Box plots showing the top ten metabolic DEGs based on the adjusted *P*-value; D: Bar plot showing top ten upregulated and downregulated Kyoto Encyclopedia of Genes and Genomes items; E: Pheatmap showing the consensus matrix (*k* = 3); F and G: Kaplan-Meier curves showing overall survival and progression free interval across three clusters. ^b*P* < 0.01. GO: Gene Ontology; KEGG: Kyoto Encyclopedia of Genes and Genomes; NOX4: Nicotinamide adenine dinucleotide phosphate oxidase 4; FC: Fold change; OS: Overall survival; PFI: Progression free interval.

(Supplementary Figure 1A). Consensus clustering of CRC samples using these dysregulated DEGs identified three clusters (Figure 1E), and each cluster had a unique gene expression pattern of dysregulated DEGs (Supplementary Figure 1B). Cluster 3 (C3) had a higher proportion of patients with a smaller tumor size (T1 + T2), lower stage (stage I + stage II), less metastasis (M0 and N0), and higher microsatellite instability (MSI) than C1 and C2 (Supplementary Figure 1C-G). In line with these results, C3 had longer OS and PFI (Figure 1F and G).

Construction and validation of prediction model using survival-related genes

We next performed a univariate test and found that 536 metabolic genes correlated with OS. LASSO regression analysis identified six gene signatures that could predict OS (Supplementary Figure 2A and B). Using multivariate Cox regression analysis, we constructed the risk score model formula as follows: $-0.38 \times \text{CPT2 expression} - 0.64 \times \text{PGM2 expression} - 0.06 \times \text{CLCA1 expression} + 0.20 \times \text{RYR2 expression} - 0.54 \times \text{ARSK expression} + 0.16 \times \text{SLC6A1 expression}$ (Supplementary Figure 2C). Next, we calculated the risk score of each patient using this formula and found that patients with high-risk scores had worse survival times in the training, test, and GEO datasets (Figure 2A and B, Supplementary Figure 2D). ROC analysis revealed that this prediction model had a high predictive efficacy across three datasets (Figure 2D and E, Supplementary Figure 2E). Next, our clinical cohort was used to validate the prediction model and clinical information was summarized in Table 1. In line with our findings, patients with high risk showed shorter survival time (Figure 2C). The prediction model showed high ROC values (Figure 2F). Univariate and multivariate analyses of the risk scores combined with several other clinical parameters revealed that risk score, age, M-stage, and N-stage were correlated with OS and could serve as independent survival risk factors in CRC (Figure 3A and B). In addition, the ROC analysis showed that the risk score had the highest sensitivity and specificity (Figure 3C). Finally, we constructed a nomogram using these independent risk scores to predict the survival of patients with CRC (Figure 3D).

NOX4 promotes tumor progression in CRC

To identify potential metabolic targets, the upregulated DEGs ($\log_{2}\text{FC} > 2.5$, adjusted *P* value < 0.05) in tumor tissues were overlapped with unfavorable survival-related genes (*P* < 0.01) (Figure 4A). Three genes were identified: NOX4, Biglycan, and phosphatidic acid phosphatase type 2 domain containing 1A. Between these three genes, NOX4 had the highest expression levels in tumor tissues (Table 2, Supplementary Figure 3A and B), indicating its potent role in promoting tumor progression. In line with these results, our clinical data demonstrated that NOX4 was highly expressed in tumor tissues at both mRNA and protein levels (Figure 4B-D). Furthermore, high NOX4 expression levels predicted a shorter OS and a higher stage of CRC (Figure 4E, Table 2). We next overexpressed NOX4 in the CRC cell line RKO (Supplementary Figure 3C-E), and found that the overexpression of NOX4 induced clone and tumorsphere formation, as well as cell migration and invasion of tumor cells (Figure 4F-J), while it had no effect on cell proliferation, cell cycle, and apoptosis (Supplementary Figure 3F-H).

NOX4 activates MAPK/MEK1/2/ERK1/2 signaling

To elucidate the NOX4-mediated signaling pathway, we performed RNA-sequencing analysis of wild-type (RKO-Ctrl) and NOX4-overexpressing RKO (RKO-OE) cells. Our results showed distinct transcriptional expression patterns in RKO-

Table 2 Three genes obtained from the intersection of differential genes and prognostic genes in colorectal cancer

Gene symbol	Log FC	HR	Function
NOX4	2.868242	1.197865	Constitutive NADPH oxidase which generates superoxide intracellularly
BGN	2.368592	1.259598	May be involved in collagen fiber assembly
PPAPDC1A	2.345055	1.126713	Magnesium-independent phospholipid phosphatase with broad substrate specificity

NOX4: Nicotinamide adenine dinucleotide phosphate oxidase 4; NADPH: Nicotinamide adenine dinucleotide phosphate; FC: Fold change; HR: Hazard ratio.

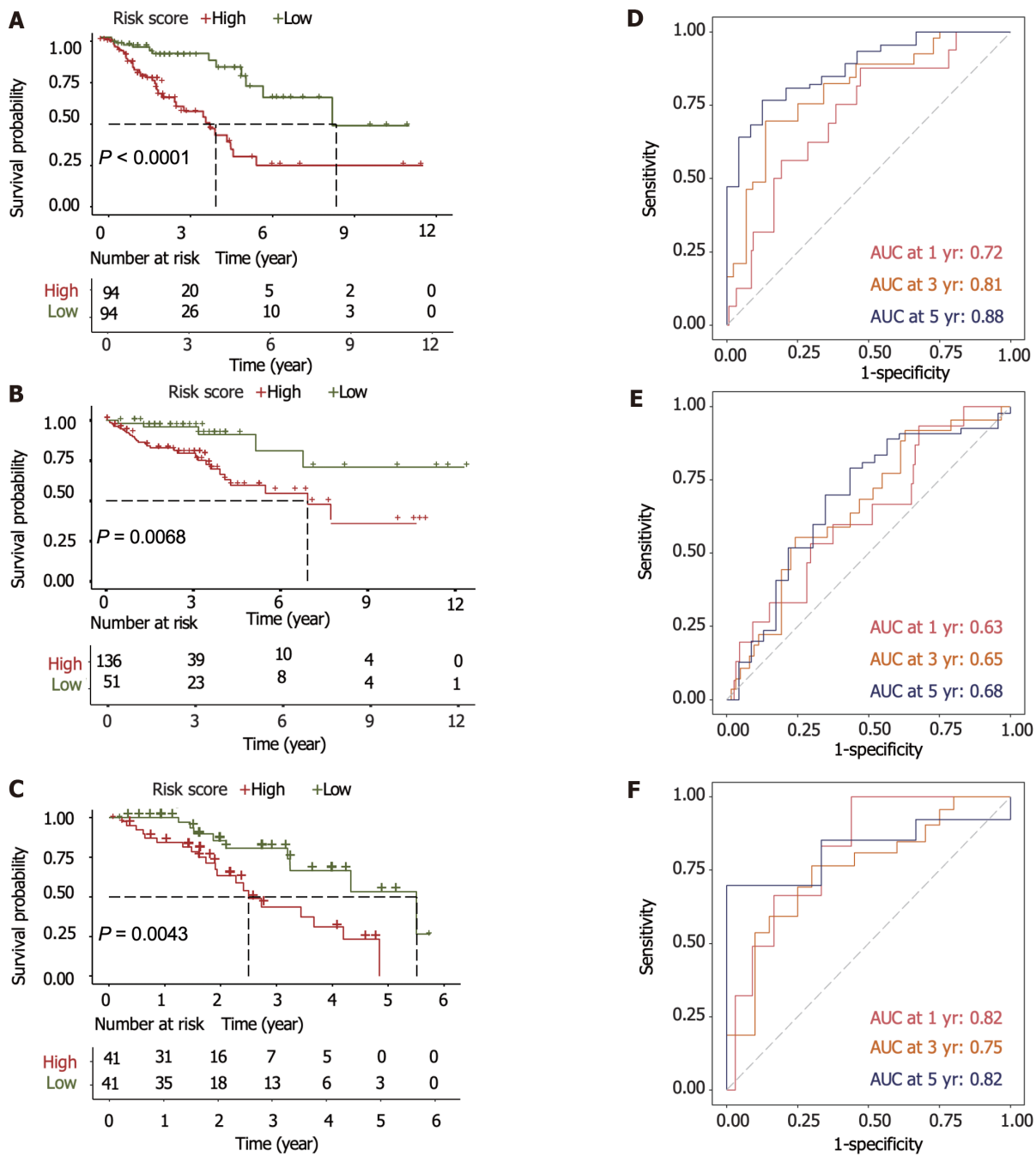


Figure 2 Construction and validation of the prediction model. A-C: Kaplan-Meier curves showing the survival differences between high and low-risk groups in training, test datasets and our clinical cohort; D-F: Receiver operating characteristic curves showing the area under curve in training, test datasets and our clinical cohort. AUC: Area under curve.

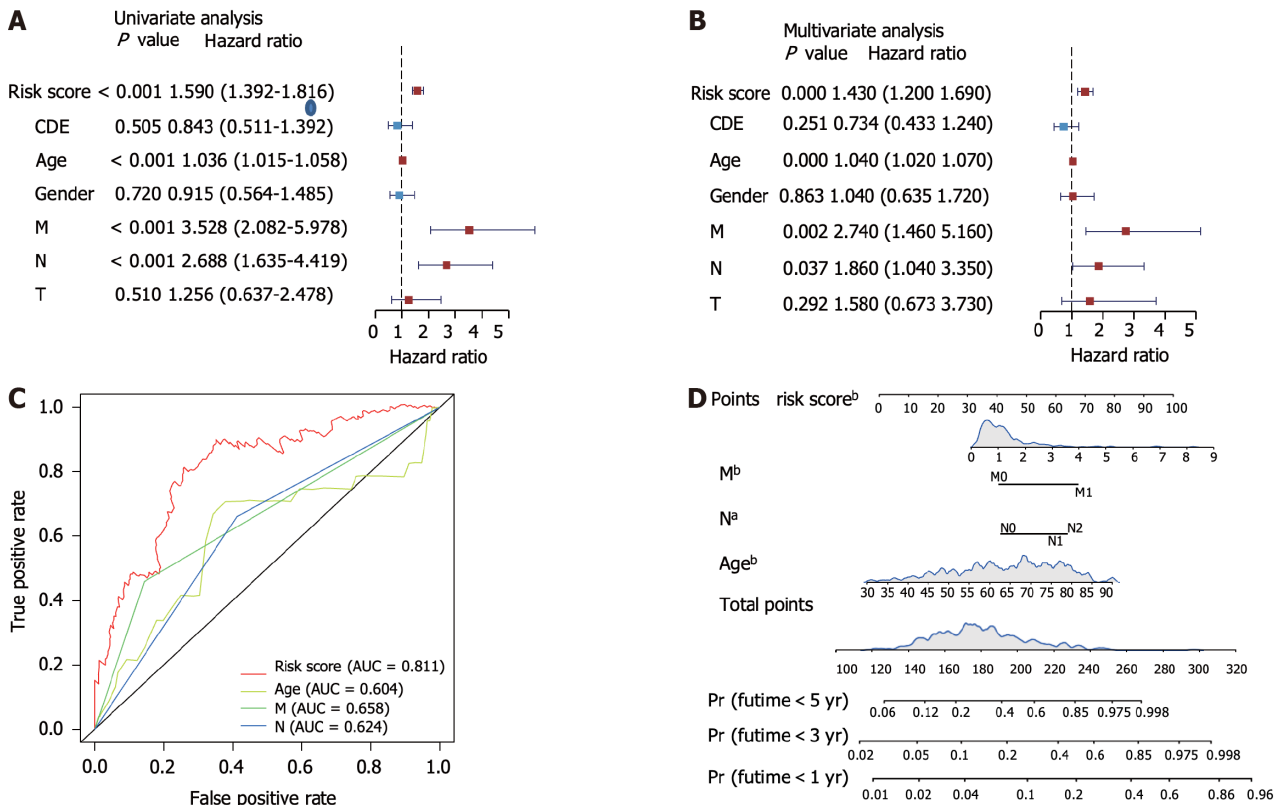


Figure 3 Validation of the risk score and survival prediction model. A and B: Forest plots showing the univariate and multivariate analysis of risk scores and other clinical parameters; C: Receiver operating characteristic analysis showing the area under curve of each factor for predicting colorectal cancer overall survival; D: Construction of nomogram using the independent risk score. ^aP < 0.05, ^bP < 0.01. AUC: Area under curve.

Ctrl and -OE cells (Figure 5A). Of the DEGs between two groups, NOX4 was the most DEG among the upregulated genes, validating our transfection efficiency (Figure 5B, Supplementary Figure 4A). GO analysis of the upregulated DEGs revealed that these genes were involved in RNA polymerase II transcription factor activity, DNA and ion binding. Furthermore, GO analysis of the downregulated genes demonstrated that DEGs were enriched in ‘protein binding’ (Supplementary Figure 4B). KEGG analysis showed that the upregulated DEGs were mostly enriched in the MAPK signal transduction pathway (Figure 5C), indicating that NOX4 could be involved in MAPK signaling. The RAS-RAF-MEK1/2-ERK1/2 axis is one of MAPK classic activation pathways[21] and our results showed that the overexpression of NOX4 increased the levels of phosphorylated MEK and its downstream target phosphorylated ERK; however, these effects were reversed by the MEK inhibitor, trametinib (Figure 5D and E). In addition, the inhibition of MAPK signaling by trametinib decreased clone formation, migration, invasion, and sphere formation in CRC cells (Figure 5F-J).

NOX4 promotes tumorigenesis and metastasis through MAPK signaling in vivo

We next constructed a subcutaneous CRC xenograft model in nude mice using RKO-Ctrl and RKO-OE cells. The results showed that NOX4 overexpression promoted subcutaneous tumor growth (Figure 6A and B). In addition, IHC analysis indicated that RKO-OE cells induced NOX4 overexpression and ERK phosphorylation in tumor tissues (Figure 6C). Meanwhile, we established a lung metastasis tumor model using a tail vein injection to evaluate the role of NOX4 in metastasis *in vivo*. Our results demonstrated that a higher number of pulmonary nodules was observed in mice injected with RKO-OE cells compared to RKO-Ctrl injected mice, whereas trametinib treatment reduced the number of NOX4-mediated metastasis (Figure 6D-F).

DISCUSSION

Metabolic reprogramming is a feature of cancer, numerous studies have shown that dysregulated metabolic process promotes CRC progression[22,23]. Herein, we identified all dysregulated metabolic genes in CRC and comprehensively analyzed their function.

CRC is heterogeneous and can be divided into several subgroups which correlate with disease prognosis and treatment efficiency. Chromosomal instability accounts for 85% of CRC and is characterized by the activation of proliferation pathways[24]. MSI involves changes in the number of short repeated sequences called microsatellites that are spread across the genome, and patients with MSI-high have longer survival rates and would benefit from immunotherapy[7]. The CpG island methylator phenotype is characterized by high levels of CpG island hypermethylation at the promoters

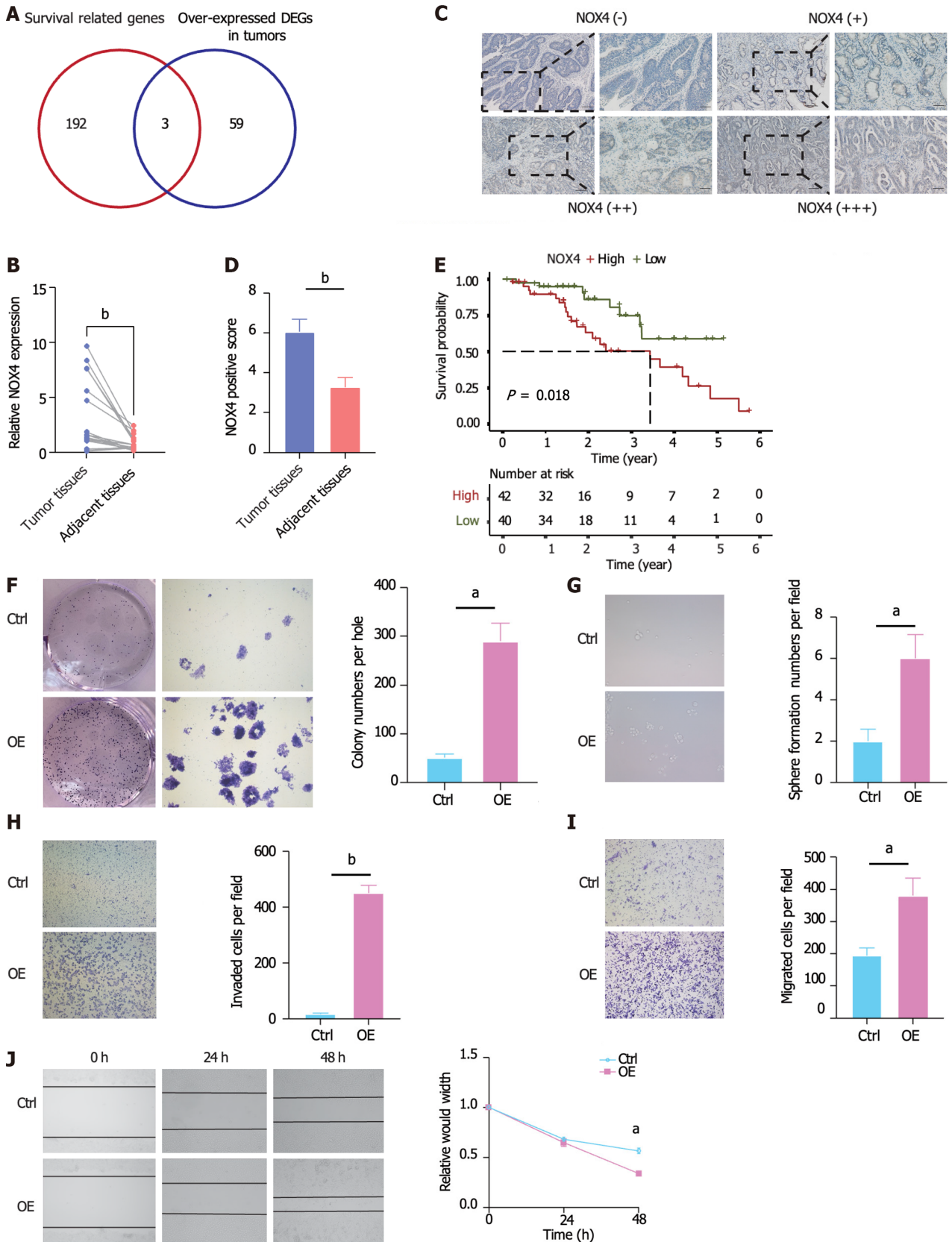


Figure 4 Nicotinamide adenine dinucleotide phosphate oxidase 4 induces colorectal cancer progression. A: Venn diagram showing the overlap of metabolic differentially expressed genes and genes correlated with poor prognosis; B: Quantitative real-time polymerase chain reaction analysis of nicotinamide adenine dinucleotide phosphate oxidase 4 (NOX4) expression in tumor and adjacent normal tissues; C: Immunohistochemical representative images of NOX4 expression in colorectal cancer patient samples; D: Quantification of NOX4 expression in tumor and adjacent normal tissues in tumor samples; E: Kaplan-Meier curves showing the overall survival between high and low-NOX4 expression groups in our dataset; F and G: Clone and sphere formation was evaluated in NOX4-overexpressing RKO (RKO-OE) and wild-type (RKO-Ctrl) cells; H-J: Cell invasion and migration of RKO-OE and RKO-Ctrl cells were measured using the transwell chamber assay and scratch assay. $^*P < 0.05$, $^{b}P < 0.01$. DEG: Differentially expressed gene; NOX4: Nicotinamide adenine dinucleotide phosphate oxidase 4.

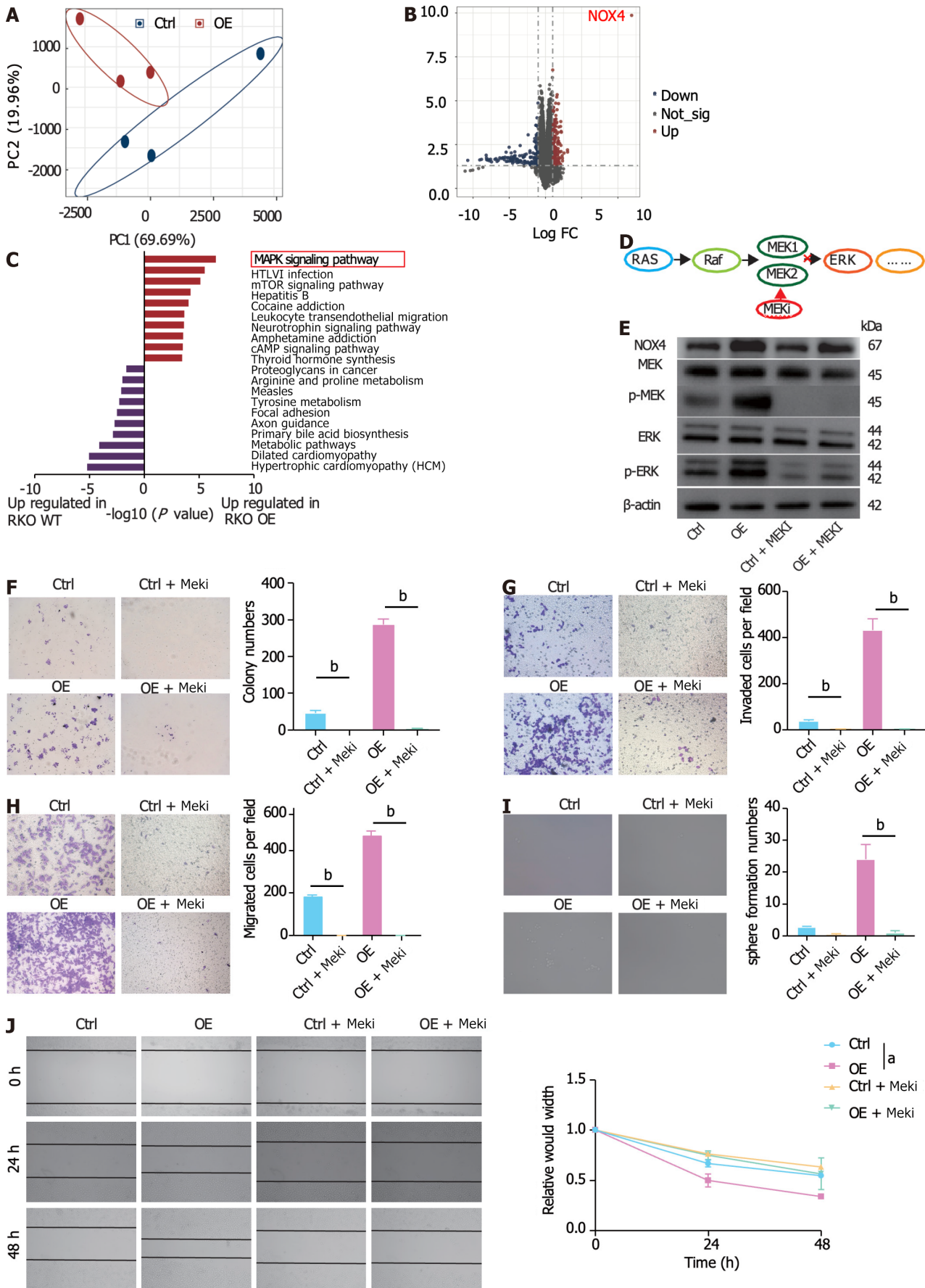


Figure 5 Nicotinamide adenine dinucleotide phosphate oxidase 4 promotes activation of mitogen-activated protein kinase/MEK1/2/ERK1/2 signaling. **A:** Principal component analysis of the transcription patterns in nicotinamide adenine dinucleotide phosphate oxidase 4 (NOX4)-

overexpressing RKO (RKO-OE) and wild-type (RKO-Ctrl) cells; B: Volcano map showing the differentially expressed genes between RKO-OE and RKO-Ctrl cells; C: Bar plot showing top ten Kyoto Encyclopedia of Genes and Genomes; D: Pattern diagram showing the RAS-RAF-MEK1/2-ERK1/2 axis; E: Western blot analysis showing the expression of NOX4, MEK, pMEK, ERK, pERK in RKO-OE and RKO-Ctrl cells, cultured with or without trametinib; F-J: Clone formation, invasion, migration, sphere formation in RKO-OE and RKO-Ctrl cells, cultured with or without trametinib. ^a*P* < 0.05, ^b*P* < 0.01. NOX4: Nicotinamide adenine dinucleotide phosphate oxidase 4; FC: Fold change; MAPK: Mitogen-activated protein kinase.

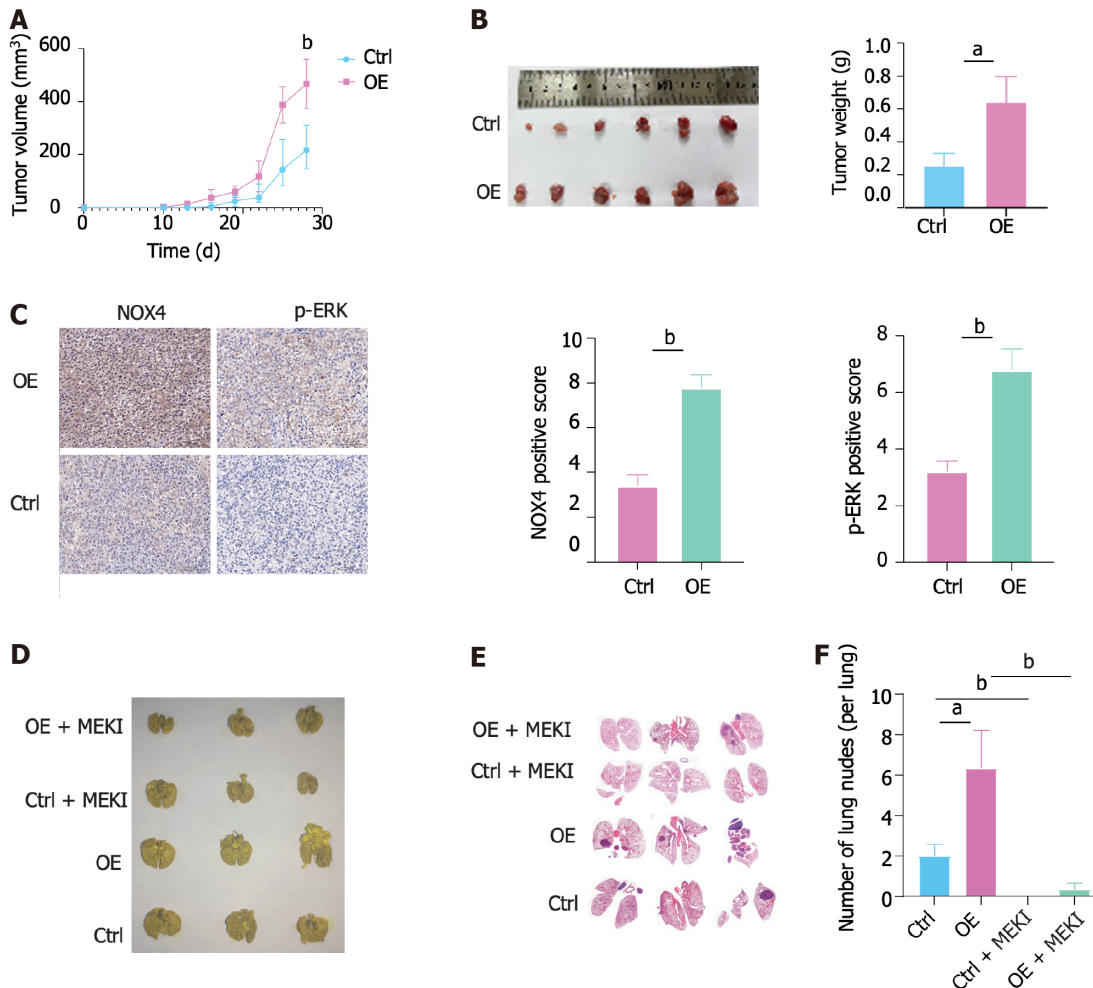


Figure 6 Nicotinamide adenine dinucleotide phosphate oxidase 4 promotes tumorigenesis and metastasis *in vivo*. A: Volume of nicotinamide adenine dinucleotide phosphate oxidase 4 (NOX4)-overexpressing RKO and wild-type tumor and measured at indicated time points; B: The representative image of subcutaneous tumors at the end of the experiment (day 28); C: Immunohistochemical staining analysis showing NOX4 and pERK expression in two groups; D: The representative image of metastatic nodes in the mouse lung tissue; E: Hematoxylin-eosin staining of tumor metastasis in mouse lung tissues; F: Quantification of tumor metastasis in lung tissues. ^a*P* < 0.05, ^b*P* < 0.01. NOX4: Nicotinamide adenine dinucleotide phosphate oxidase 4.

of several tumor suppressor genes[25]. Guinney *et al*[26] used a large gene expression dataset to identify four molecular subtypes called consensus molecular subtypes. Herein, we observed remarkable differences in prognosis of patients with CRC who were subgrouped by metabolic genes, indicating that metabolic classification is an important method for defining heterogeneity. For example, Xiao *et al*[27] generated a large metabolomic atlas of triple-negative breast cancers and classified these triple-negative breast cancers into three distinct metabolomic subgroups, while Liu *et al*[28] identified two CRC immune phenotypes using consensus clustering of immune-related gene expression profiles. Song *et al*[29] used survival-related N6-methyladenosine (m6A)-modified Long non-coding RNAs to classify CRC and to identify two subtypes. These results, combined with our findings, revealed a different perspective on CRC heterogeneity.

NOX4 plays a central role in generating ROS to facilitate tumor progression in several types of cancers. NOX4 has been identified as a modulator of two oncogenic signaling pathways, hypoxia inducible factor 1 signaling and AMP-activated protein kinase signaling[30,31]. In this study, we found that NOX4 was overexpressed in tumor tissues. Similar findings describing the role of NOX4 in CRC have been previously reported[32,33]. NOX4 overexpression in CRC cells upregulated clone formation, stemness, migration, and invasion *in vitro*, but had no effects on cell proliferation and apoptosis. The overexpression of NOX4 increased subcutaneous tumor volume and weight *in vivo*, which could have been caused by the enhanced ability to form clones and augment stemness. We also observed that NOX4 overexpression increased lung metastasis *in vivo*. Shen *et al*[34] reported that angiotensin-like 4 induced the expression of NOX4 to

promote CRC metastasis, while Cho *et al*[35] analyzed the expression of the NOX family and found that NOX4 expression levels were related to the degree of tumor malignancy. Mechanistically, we found that NOX4 activates the MAPK/MEK1/2/ERK1/2 signaling pathway. MAPKs are well-known oncogenic signaling molecules involved in tumor progression[36]. Mutations and the overexpression of genes involved in MAPK signaling have been frequently observed in CRC[37]. Previous studies have shown that NOX4 can activate MAPK signaling in pancreatic carcinoma and breast cancer[38,39]. In our study, RNA-sequencing analysis results showed that the overexpression of NOX4 activated MAPK signaling, and *in vitro* and *in vivo* analyses demonstrated that the inhibition of MAPK signaling (trametinib) abolished NOX4-mediated tumor growth and metastasis. Our findings further demonstrated the correlation between NOX4 expression and MAPK signaling and highlighted trametinib targeting NOX4 to inhibit MAPK signaling in CRC.

In summary, our *in vitro* and *in vivo* studies have explored the tumorigenic functions of NOX4 and downstream MAPK signaling. Our results suggest that NOX4 induces tumor progression and, therefore, could be used as a potential metabolic target in CRC.

CONCLUSION

In this study, we identified metabolic DEGs and comprehensively explored their expression and function in CRC. The CRC clusters based on dysregulated metabolic genes provided a novel insight into the heterogeneity of CRC. A prediction model generated using metabolic gene signatures could be used to predict patient prognosis. In summary, our *in vitro* and *in vivo* studies have explored the tumorigenic functions of NOX4 and downstream MAPK signaling. Our results suggest that NOX4 induces tumor progression and, therefore, could be used as a potential metabolic target in CRC.

ARTICLE HIGHLIGHTS

Research background

Colorectal cancer (CRC) is the leading cause of cancer-related death. Although conventional therapy has improved the prognosis of CRC, majority of patient do not well respond to these therapies. Therefore, identification of new targets is urgent for CRC.

Research motivation

Metabolic reprogramming is the major cause of therapy failure. In this study, we aim to explore the metabolic alteration in CRC tumor tissue and identify the key metabolic genes mediated this process.

Research objectives

We aim to explore the differently expressed metabolic genes between tumor and normal tissue as well as correlated with survival. In addition, we want to construct a prediction model based on this metabolic gene and identify key metabolic genes.

Research methods

We used bioinformatics analysis to identify differently expressed genes and survival related genes. Cox regression model was used to construct prediction model. Tumor biology experiments and *in vivo* mouse model were used to validate the role of nicotinamide adenine dinucleotide phosphate oxidase 4 (NOX4) in mediating CRC progression.

Research results

We found that most of metabolic genes were dys-regulated between tumor and normal tissue. The NOX4 was the key metabolic gene that promoted proliferation, migration invasion and stemness of tumor cell through mitogen-activated protein kinase signaling pathway. *In vivo* mouse models, over-expression of NOX4 increased tumor growth and metastasis.

Research conclusions

NOX4 is a key metabolic gene that promote CRC progression.

Research perspectives

Combined therapies with targeting NOX4 may be a promising strategy for CRC treatment.

FOOTNOTES

Co-first authors: Yu-Jie Xu and Ya-Chang Huo.

Author contributions: Xu YJ and Huo YC equally contributed to this work. Xu YJ, Huo YC, and Zhao QT analyzed the data; Xu YJ

performed the experiments and drafted the manuscript; Huo YC and Zhao QT prepared the figures; Liu JY and Tian YJ performed hematoxylin-eosin and immunohistochemical staining experiments; Yang LL corrected the figures; Zhang Y designed, supervised and supported the study, and edited the manuscript; and all authors have read and approve the final the manuscript.

Supported by Henan Province Medical Science and Technology Research Provincial and Ministry Co-constructed Projects, No. SBGJ202101010; Major Public Welfare Projects in Henan Province, No. 201300310400; Joint Construction Project of Henan Medical Science and Technology Research Plan, No. LHGJ20220050; and Major Science and Technology Project of Henan Province, No. 221100310100.

Institutional review board statement: Approval of the research protocol by the Committee of First Affiliated Hospital of Zhengzhou University (No. 2022-KY-0828-003).

Clinical trial registration statement: This manuscript is not a Clinical Trial. The clinical part in the manuscript is a retrospective analysis. So we don't have a clinical trial registration statement.

Conflict-of-interest statement: All the authors report no relevant conflicts of interest for this article.

Data sharing statement: All public data can be downloaded from TCGA through online database UCSC Xena (xena.ucsc.edu) and GEO using the access number: GSE17536. Other data used in the study are available from the corresponding author upon reasonable request.

Open-Access: This article is an open-access article that was selected by an in-house editor and fully peer-reviewed by external reviewers. It is distributed in accordance with the Creative Commons Attribution NonCommercial (CC BY-NC 4.0) license, which permits others to distribute, remix, adapt, build upon this work non-commercially, and license their derivative works on different terms, provided the original work is properly cited and the use is non-commercial. See: <https://creativecommons.org/licenses/by-nc/4.0/>

Country/Territory of origin: China

ORCID number: Yi Zhang [0000-0001-9861-4681](https://orcid.org/0000-0001-9861-4681).

S-Editor: Wang JJ

L-Editor: A

P-Editor: Zhang XD

REFERENCES

- 1 **Dekker E**, Tanis PJ, Vleugels JLA, Kasi PM, Wallace MB. Colorectal cancer. *Lancet* 2019; **394**: 1467-1480 [PMID: [31631858](https://pubmed.ncbi.nlm.nih.gov/31631858/) DOI: [10.1016/S0140-6736\(19\)32319-0](https://doi.org/10.1016/S0140-6736(19)32319-0)]
- 2 **Hayashi N**, Tanaka S, Hewett DG, Kaltenbach TR, Sano Y, Ponchon T, Saunders BP, Rex DK, Soetikno RM. Endoscopic prediction of deep submucosal invasive carcinoma: validation of the narrow-band imaging international colorectal endoscopic (NICE) classification. *Gastrointest Endosc* 2013; **78**: 625-632 [PMID: [23910062](https://pubmed.ncbi.nlm.nih.gov/23910062/) DOI: [10.1016/j.gie.2013.04.185](https://doi.org/10.1016/j.gie.2013.04.185)]
- 3 **Jayanna M**, Burgess NG, Singh R, Hourigan LF, Brown GJ, Zanati SA, Moss A, Lim J, Sonson R, Williams SJ, Bourke MJ. Cost Analysis of Endoscopic Mucosal Resection vs Surgery for Large Laterally Spreading Colorectal Lesions. *Clin Gastroenterol Hepatol* 2016; **14**: 271-8.e1 [PMID: [26364679](https://pubmed.ncbi.nlm.nih.gov/26364679/) DOI: [10.1016/j.cgh.2015.08.037](https://doi.org/10.1016/j.cgh.2015.08.037)]
- 4 **Taylor FG**, Quirke P, Heald RJ, Moran B, Blomqvist L, Swift I, Sebag-Montefiore DJ, Tekkis P, Brown G; MERCURY study group. Preoperative high-resolution magnetic resonance imaging can identify good prognosis stage I, II, and III rectal cancer best managed by surgery alone: a prospective, multicenter, European study. *Ann Surg* 2011; **253**: 711-719 [PMID: [21475011](https://pubmed.ncbi.nlm.nih.gov/21475011/) DOI: [10.1097/SLA.0b013e31820b8d52](https://doi.org/10.1097/SLA.0b013e31820b8d52)]
- 5 **Schmoll HJ**, Tabernero J, Maroun J, de Braud F, Price T, Van Cutsem E, Hill M, Hoersch S, Rittweger K, Haller DG. Capecitabine Plus Oxaliplatin Compared With Fluorouracil/Folinic Acid As Adjuvant Therapy for Stage III Colon Cancer: Final Results of the NO16968 Randomized Controlled Phase III Trial. *J Clin Oncol* 2015; **33**: 3733-3740 [PMID: [26324362](https://pubmed.ncbi.nlm.nih.gov/26324362/) DOI: [10.1200/JCO.2015.60.9107](https://doi.org/10.1200/JCO.2015.60.9107)]
- 6 **Cunningham D**, Lang I, Marcuello E, Lorusso V, Ocvirk J, Shin DB, Jonker D, Osborne S, Andre N, Waterkamp D, Saunders MP; AVEX study investigators. Bevacizumab plus capecitabine versus capecitabine alone in elderly patients with previously untreated metastatic colorectal cancer (AVEX): an open-label, randomised phase 3 trial. *Lancet Oncol* 2013; **14**: 1077-1085 [PMID: [24028813](https://pubmed.ncbi.nlm.nih.gov/24028813/) DOI: [10.1016/S1470-2045\(13\)70154-2](https://doi.org/10.1016/S1470-2045(13)70154-2)]
- 7 **Ganesh K**, Stadler ZK, Cercek A, Mendelsohn RB, Shia J, Segal NH, Diaz LA Jr. Immunotherapy in colorectal cancer: rationale, challenges and potential. *Nat Rev Gastroenterol Hepatol* 2019; **16**: 361-375 [PMID: [30886395](https://pubmed.ncbi.nlm.nih.gov/30886395/) DOI: [10.1038/s41575-019-0126-x](https://doi.org/10.1038/s41575-019-0126-x)]
- 8 **Luo M**, Yang X, Chen HN, Nice EC, Huang C. Drug resistance in colorectal cancer: An epigenetic overview. *Biochim Biophys Acta Rev Cancer* 2021; **1876**: 188623 [PMID: [34481016](https://pubmed.ncbi.nlm.nih.gov/34481016/) DOI: [10.1016/j.bbcan.2021.188623](https://doi.org/10.1016/j.bbcan.2021.188623)]
- 9 **Hanahan D**, Weinberg RA. Hallmarks of cancer: the next generation. *Cell* 2011; **144**: 646-674 [PMID: [21376230](https://pubmed.ncbi.nlm.nih.gov/21376230/) DOI: [10.1016/j.cell.2011.02.013](https://doi.org/10.1016/j.cell.2011.02.013)]
- 10 **Martínez-Reyes I**, Chandel NS. Cancer metabolism: looking forward. *Nat Rev Cancer* 2021; **21**: 669-680 [PMID: [34272515](https://pubmed.ncbi.nlm.nih.gov/34272515/) DOI: [10.1038/s41568-021-00378-6](https://doi.org/10.1038/s41568-021-00378-6)]
- 11 **WARBURG O**. On respiratory impairment in cancer cells. *Science* 1956; **124**: 269-270 [PMID: [13351639](https://pubmed.ncbi.nlm.nih.gov/13351639/)]
- 12 **Vaupel P**, Schmidberger H, Mayer A. The Warburg effect: essential part of metabolic reprogramming and central contributor to cancer progression. *Int J Radiat Biol* 2019; **95**: 912-919 [PMID: [30822194](https://pubmed.ncbi.nlm.nih.gov/30822194/) DOI: [10.1080/09553002.2019.1589653](https://doi.org/10.1080/09553002.2019.1589653)]
- 13 **Najumudeen AK**, Ceteci F, Fey SK, Hamm G, Steven RT, Hall H, Nikula CJ, Dexter A, Murta T, Race AM, Sumpton D, Vlahov N, Gay DM, Knight JRP, Jackstadt R, Leach JDG, Ridgway RA, Johnson ER, Nixon C, Hedley A, Gilroy K, Clark W, Malla SB, Dunne PD, Rodriguez-

- Blanco G, Critchlow SE, Mrowinska A, Malviya G, Solovyev D, Brown G, Lewis DY, Mackay GM, Strathdee D, Tardito S, Gottlieb E; CRUK Rosetta Grand Challenge Consortium, Takats Z, Barry ST, Goodwin RJA, Bunch J, Bushell M, Campbell AD, Sansom OJ. The amino acid transporter SLC7A5 is required for efficient growth of KRAS-mutant colorectal cancer. *Nat Genet* 2021; **53**: 16-26 [PMID: 33414552 DOI: 10.1038/s41588-020-00753-3]
- 14 **Schulte ML**, Fu A, Zhao P, Li J, Geng L, Smith ST, Kondo J, Coffey RJ, Johnson MO, Rathmell JC, Sharick JT, Skala MC, Smith JA, Berlin J, Washington MK, Nickels ML, Manning HC. Pharmacological blockade of ASCT2-dependent glutamine transport leads to antitumor efficacy in preclinical models. *Nat Med* 2018; **24**: 194-202 [PMID: 29334372 DOI: 10.1038/nm.4464]
- 15 **Edwards DN**, Ngwa VM, Raybuck AL, Wang S, Hwang Y, Kim LC, Cho SH, Paik Y, Wang Q, Zhang S, Manning HC, Rathmell JC, Cook RS, Boothby MR, Chen J. Selective glutamine metabolism inhibition in tumor cells improves antitumor T lymphocyte activity in triple-negative breast cancer. *J Clin Invest* 2021; **131** [PMID: 33320840 DOI: 10.1172/JCI140100]
- 16 **Szanto I**. NADPH Oxidase 4 (NOX4) in Cancer: Linking Redox Signals to Oncogenic Metabolic Adaptation. *Int J Mol Sci* 2022; **23** [PMID: 35269843 DOI: 10.3390/ijms23052702]
- 17 **Tang CT**, Gao YJ, Ge ZZ. NOX4, a new genetic target for anti-cancer therapy in digestive system cancer. *J Dig Dis* 2018; **19**: 578-585 [PMID: 30058122 DOI: 10.1111/1751-2980.12651]
- 18 **Vermot A**, Petit-Härtlein I, Smith SME, Fieschi F. NADPH Oxidases (NOX): An Overview from Discovery, Molecular Mechanisms to Physiology and Pathology. *Antioxidants (Basel)* 2021; **10** [PMID: 34205998 DOI: 10.3390/antiox10060890]
- 19 **Haider S**, McIntyre A, van Stiphout RG, Winchester LM, Wigfield S, Harris AL, Buffa FM. Genomic alterations underlie a pan-cancer metabolic shift associated with tumour hypoxia. *Genome Biol* 2016; **17**: 140 [PMID: 27358048 DOI: 10.1186/s13059-016-0999-8]
- 20 **Peng X**, Chen Z, Farshidfar F, Xu X, Lorenzi PL, Wang Y, Cheng F, Tan L, Mojumdar K, Du D, Ge Z, Li J, Thomas GV, Birsoy K, Liu L, Zhang H, Zhao Z, Marchand C, Weinstein JN; Cancer Genome Atlas Research Network, Bathe OF, Liang H. Molecular Characterization and Clinical Relevance of Metabolic Expression Subtypes in Human Cancers. *Cell Rep* 2018; **23**: 255-269.e4 [PMID: 29617665 DOI: 10.1016/j.celrep.2018.03.077]
- 21 **Tsai HC**, Tsou HH, Lin CC, Chen SC, Cheng HW, Liu TY, Chen WS, Jiang JK, Yang SH, Chang SC, Teng HW, Wang HT. Acrolein contributes to human colorectal tumorigenesis through the activation of RAS-MAPK pathway. *Sci Rep* 2021; **11**: 12590 [PMID: 34131238 DOI: 10.1038/s41598-021-92035-z]
- 22 **Coleman O**, Ecker M, Haller D. Dysregulated lipid metabolism in colorectal cancer. *Curr Opin Gastroenterol* 2022; **38**: 162-167 [PMID: 35098938 DOI: 10.1097/MOG.0000000000000811]
- 23 **Mika A**, Duzowska K, Halinski LP, Pakiet A, Czumaj A, Rostkowska O, Dobrzycka M, Kobiela J, Sledzinski T. Rearrangements of Blood and Tissue Fatty Acid Profile in Colorectal Cancer - Molecular Mechanism and Diagnostic Potential. *Front Oncol* 2021; **11**: 689701 [PMID: 34123858 DOI: 10.3389/fonc.2021.689701]
- 24 **Geigl JB**, Obenaus AC, Schwarzbraun T, Speicher MR. Defining 'chromosomal instability'. *Trends Genet* 2008; **24**: 64-69 [PMID: 18192061 DOI: 10.1016/j.tig.2007.11.006]
- 25 **Weisenberger DJ**, Siegmund KD, Campan M, Young J, Long TI, Faasse MA, Kang GH, Widschwendter M, Weener D, Buchanan D, Koh H, Simms L, Barker M, Leggett B, Levine J, Kim M, French AJ, Thibodeau SN, Jass J, Haile R, Laird PW. CpG island methylator phenotype underlies sporadic microsatellite instability and is tightly associated with BRAF mutation in colorectal cancer. *Nat Genet* 2006; **38**: 787-793 [PMID: 16804544 DOI: 10.1038/ng1834]
- 26 **Guinney J**, Dienstmann R, Wang X, de Reyniès A, Schlicker A, Soneson C, Marisa L, Roepman P, Nyamundanda G, Angelino P, Bot BM, Morris JS, Simon IM, Gerster S, Fessler E, De Sousa E Melo F, Missiaglia E, Ramay H, Barras D, Homicsko K, Maru D, Manyam GC, Broom B, Boige V, Perez-Villamil B, Laderas T, Salazar R, Gray JW, Hanahan D, Tabernero J, Bernards R, Friend SH, Laurent-Puig P, Medema JP, Sadanandam A, Wessels L, Delorenzi M, Kopetz S, Vermeulen L, Tejpar S. The consensus molecular subtypes of colorectal cancer. *Nat Med* 2015; **21**: 1350-1356 [PMID: 26457759 DOI: 10.1038/nm.3967]
- 27 **Xiao Y**, Ma D, Yang YS, Yang F, Ding JH, Gong Y, Jiang L, Ge LP, Wu SY, Yu Q, Zhang Q, Bertucci F, Sun Q, Hu X, Li DQ, Shao ZM, Jiang YZ. Comprehensive metabolomics expands precision medicine for triple-negative breast cancer. *Cell Res* 2022; **32**: 477-490 [PMID: 35105939 DOI: 10.1038/s41422-022-00614-0]
- 28 **Liu Z**, Guo Y, Yang X, Chen C, Fan D, Wu X, Si C, Xu Y, Shao B, Chen Z, Dang Q, Cui W, Han X, Ji Z, Sun Z. Immune Landscape Refines the Classification of Colorectal Cancer With Heterogeneous Prognosis, Tumor Microenvironment and Distinct Sensitivity to Frontline Therapies. *Front Cell Dev Biol* 2021; **9**: 784199 [PMID: 35083217 DOI: 10.3389/fcell.2021.784199]
- 29 **Song W**, Ren J, Yuan W, Xiang R, Ge Y, Fu T. N6-Methyladenosine-Related lncRNA Signature Predicts the Overall Survival of Colorectal Cancer Patients. *Genes (Basel)* 2021; **12** [PMID: 34573357 DOI: 10.3390/genes12091375]
- 30 **Semenza GL**. HIF-1 mediates metabolic responses to intratumoral hypoxia and oncogenic mutations. *J Clin Invest* 2013; **123**: 3664-3671 [PMID: 23999440 DOI: 10.1172/JCI167230]
- 31 **Faubert B**, Vincent EE, Poffenberger MC, Jones RG. The AMP-activated protein kinase (AMPK) and cancer: many faces of a metabolic regulator. *Cancer Lett* 2015; **356**: 165-170 [PMID: 24486219 DOI: 10.1016/j.canlet.2014.01.018]
- 32 **Ford K**, Hanley CJ, Mellone M, Szyndralewicz C, Heitz F, Wiesel P, Wood O, Machado M, Lopez MA, Ganesan AP, Wang C, Chakravarthy A, Fenton TR, King EV, Vijayanand P, Ottensmeier CH, Al-Shamkhani A, Savelyeva N, Thomas GJ. NOX4 Inhibition Potentiates Immunotherapy by Overcoming Cancer-Associated Fibroblast-Mediated CD8 T-cell Exclusion from Tumors. *Cancer Res* 2020; **80**: 1846-1860 [PMID: 32122909 DOI: 10.1158/0008-5472.CAN-19-3158]
- 33 **Lin XL**, Yang L, Fu SW, Lin WF, Gao YJ, Chen HY, Ge ZZ. Overexpression of NOX4 predicts poor prognosis and promotes tumor progression in human colorectal cancer. *Oncotarget* 2017; **8**: 33586-33600 [PMID: 28422720 DOI: 10.18632/oncotarget.16829]
- 34 **Shen CJ**, Chang KY, Lin BW, Lin WT, Su CM, Tsai JP, Liao YH, Hung LY, Chang WC, Chen BK. Oleic acid-induced NOX4 is dependent on ANGPTL4 expression to promote human colorectal cancer metastasis. *Theranostics* 2020; **10**: 7083-7099 [PMID: 32641980 DOI: 10.7150/thno.44744]
- 35 **Cho SY**, Kim JS, Eun HS, Kang SH, Lee ES, Kim SH, Sung JK, Lee BS, Jeong HY, Moon HS. Expression of NOX Family Genes and Their Clinical Significance in Colorectal Cancer. *Dig Dis Sci* 2018; **63**: 2332-2340 [PMID: 29781053 DOI: 10.1007/s10620-018-5121-5]
- 36 **Guo YJ**, Pan WW, Liu SB, Shen ZF, Xu Y, Hu LL. ERK/MAPK signalling pathway and tumorigenesis. *Exp Ther Med* 2020; **19**: 1997-2007 [PMID: 32104259 DOI: 10.3892/etm.2020.8454]
- 37 **Stefani C**, Miricescu D, Stanescu-Spinu II, Nica RI, Greabu M, Totan AR, Jinga M. Growth Factors, PI3K/AKT/mTOR and MAPK Signaling Pathways in Colorectal Cancer Pathogenesis: Where Are We Now? *Int J Mol Sci* 2021; **22** [PMID: 34638601 DOI: 10.3390/ijms221910260]

- 38 **Witte D**, Bartscht T, Kaufmann R, Pries R, Settmacher U, Lehnert H, Ungefroren H. TGF- β 1-induced cell migration in pancreatic carcinoma cells is RAC1 and NOX4-dependent and requires RAC1 and NOX4-dependent activation of p38 MAPK. *Oncol Rep* 2017; **38**: 3693-3701 [PMID: 29039574 DOI: 10.3892/or.2017.6027]
- 39 **Chiou JT**, Shi YJ, Lee YC, Wang LJ, Chen YJ, Chang LS. Carboxyl group-modified α -lactalbumin induces TNF- α -mediated apoptosis in leukemia and breast cancer cells through the NOX4/p38 MAPK/PP2A axis. *Int J Biol Macromol* 2021; **187**: 513-527 [PMID: 34310992 DOI: 10.1016/j.ijbiomac.2021.07.133]



Published by **Baishideng Publishing Group Inc**
7041 Koll Center Parkway, Suite 160, Pleasanton, CA 94566, USA
Telephone: +1-925-3991568
E-mail: office@baishideng.com
Help Desk: <https://www.f6publishing.com/helpdesk>
<https://www.wjgnet.com>

